Drug Development and Industrial Pharmacy

ISSN: 0363-9045 (Print) 1520-5762 (Online) Journal homepage: https://www.tandfonline.com/loi/iddi20

Formulation development and in vitro evaluation of didanosine-loaded nanostructured lipid carriers for the potential treatment of AIDS dementia complex

Kasongo Wa Kasongo, Ranjita Shegokar, Rainer H. Müller & Roderick B. Walker

To cite this article: Kasongo Wa Kasongo, Ranjita Shegokar, Rainer H. Müller & Roderick B. Walker (2011) Formulation development and in vitro evaluation of didanosine-loaded nanostructured lipid carriers for the potential treatment of AIDS dementia complex, Drug Development and Industrial Pharmacy, 37:4, 396-407, DOI: 10.3109/03639045.2010.516264

To link to this article: https://doi.org/10.3109/03639045.2010.516264

Published online: 06 Oct 2010.

Drug Development and Industrial Pharmacy, 2011, 37(4): 396–407

ISSN 0363-9045 print/ISSN 1520-5762 online
DOI:10.3109/03639045.2010.516264

informa
healthcare

ORIGINAL ARTICLE

Formulation development and in vitro evaluation of didanosine-loaded nanostructured lipid carriers for the potential treatment of AIDS dementia complex

Kasongo Wa Kasongo[1,2], Ranjita Shegokar[1], Rainer H. Müller[1] and Roderick B. Walker[2]

[1]Department of Pharmaceutics, Biopharmaceutics and NutriCosmetics, Free University of Berlin, Berlin, Germany and [2]Division of Pharmaceutics, Faculty of Pharmacy, Rhodes University, Grahamstown, South Africa

Abstract

The purpose of this article was to investigate the feasibility of incorporating didanosine (DDI) into nanostructured lipid carriers (NLC) for potential treatment of AIDS dementia complex. Aqueous DDI-free and DDI-loaded NLC were manufactured using hot high-pressure homogenization. The lipid matrix contained a mixture of Precirol® ATO 5 and Transcutol® HP. Photon correlation spectroscopy revealed that the mean particle size for all formulations was below 250 nm with narrow polydispersity indices. In addition, the d99% values for all formulations determined using laser diffractometry were below 400 nm with the span values ranging from 0.84 to 1.0. The zeta potential values ranged from –18.4 to –11.4 mV and the encapsulation efficiency of NLC for DDI ranged from 33.02% to 78.34%. These parameters remained relatively constant for all formulations tested following storage for 2 months at 25°C indicating that all the formulations were relatively stable. Differential scanning calorimetry revealed a decrease in the degree of crystallinity of NLC in all formulations developed relative to the bulk lipid material. In addition, wide-angle X-ray scattering showed that NLC in all formulations tested existed in a single β-modification form and that DDI that had been incorporated into the NLC appeared to be molecularly dispersed in the lipid matrices. Images of the NLC formulations obtained using transmission electron microscopy revealed that all formulations contained a mixture of spherical and nonspherical particles irrespective of the amount of DDI that was added during the manufacture of the formulations.

Key words: Brain dementia complex, didanosine, nanostructured lipid carriers, polymorphism and crystallinity, thermal stability

Introduction

Didanosine (2′,3′-dideoxyinosine, DDI) is a dideoxy synthetic analog of the purine nucleoside inosine (Figure 1) that has been reported to inhibit the replication of the human immunodeficiency virus (HIV)[1–5]. DDI acts as a competitive inhibitor of HIV reverse transcriptase or as a DNA chain terminator following intracellular phosphorylation to the active triphosphate, namely, 2′,3′-dideoxyadenosine-5′-triphosphate[1–5]. The drug is approved by the US Food and Drug Administration for the treatment of adult and pediatric patients older than 6 months of age[1,5]. DDI is usually indicated for patients who are presented with advanced HIV infection and who are intolerant to zidovudine or have demonstrated significant clinical or immunologic deterioration during zidovudine therapy[1,5].

HIV is the etiologic agent of acquired immunodeficiency syndrome (AIDS) and related complications such as AIDS dementia complex (ADC)[6,7]. ADC is a debilitating syndrome usually characterized by progressive degeneration of specific cognitive and psychomotor functions[6,7]. The initial phase of ADC is characterized by a deterioration in memory, attention, and concentration, which is followed by the late onset of spasticity, paraparesis, mutism, and psychosis[8]. In addition, mental slowness, reduced rates of speech, and changes in speaking volume are features of the late stages of ADC[9–11]. Clearly, the syndrome may impart negatively on the quality of

Address for correspondence: Prof. Roderick B.Walker, Division of Pharmaceutics, Faculty of Pharmacy, Rhodes University, P.O. Box 94, Grahamstown 6140, South Africa. Tel: +27466038381, Fax: +27466361205. E-mail: r.b.walker@ru.ac.za

(Received 29 Apr 2010; accepted 11 Aug 2010)

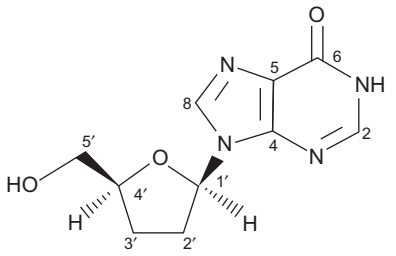

Figure 1. Structure of DDI.

life of HIV/AIDS patients and it has been intimated that HIV/AIDS patients have a one in four chance of eventually developing ADC[12].

The main cause of ADC is migration, followed by replication and accumulation of the HIV in the central nervous system (CNS). The HIV actively invades the CNS and the microglial cells in the brain reportedly serve as the most important reservoirs of the virus[13]. Dideoxynucleosides like DDI are apparently inefficient at crossing the blood–brain barrier (BBB) and maintaining sufficient therapeutic concentrations in the affected brain structures[6]. Consequently, HIV is able to multiply and accumulate in the CNS unabatedly, leading to the onset of ADC. It is therefore inevitable that adequate management of HIV infection and inhibition of viral replication within the CNS structures would require the use of drug delivery systems with the ability to deliver anti-HIV agents to the CNS by circumventing or facilitating transport across the BBB.

Innovative solid lipid carriers, such as solid lipid nanoparticles (SLN)[14–18] and nanostructured lipid carriers (NLC)[19–22] are promising drug delivery systems. SLN and NLC are alternative colloidal drug carrier systems to emulsions, liposomes, and polymeric nanoparticles[16,18] and consist of a matrix of lipid, which are solid at both room- and body temperatures and that have a mean particle size (PS) of between 50 and 1000 nm[15,18,23]. The primary difference between SLN and NLC is that the latter are prepared by mixing solid lipids with liquid lipids rather than highly purified lipids with a relatively similar molecular structure, as that used in SLN formulation[19,23]. Consequently, NLC matrices consist of a less-ordered lipid matrix with imperfections, which may lead to an increase in drug-loading capacity and prevent drug expulsion during prolonged storage periods[19–23].

SLN and NLC combine the advantages of polymeric particles, fat emulsions, and liposomes while minimizing their shortcomings[16,17]. Several advantages of using SLN and NLC include the achievement of controlled release and an improvement in the stability and bioavailability of drugs incorporated in these systems[19,22,24]. Furthermore, SLN and NLC are prepared using physiologically acceptable and biodegradable lipid materials that have GRAS (generally regarded as safe) status, while avoiding the use of organic solvents[17,19]. SLN and NLC can incorporate both hydrophilic and hydrophobic drugs under optimized conditions[22,24]. In addition, SLN and NLC can be manufactured on an industrial large scale, which is a prerequisite for commercialization[16,17]. Well-designed solid lipid carriers such as SLN have the potential to allow the penetration of nontransportable substances to the brain by masking their otherwise undesirable physicochemical properties[24–26]. Therefore, the objective of these studies was to investigate the feasibility of incorporating DDI in NLC, which could potentially be used as a vehicle for the delivery of DDI to the brain and subsequent management of ADC and improvement of the quality of life of HIV/AIDS patients.

Materials and methods

Materials

DDI was donated by Aspen Pharmacare Holdings Limited (Port Elizabeth, Eastern Cape, South Africa). The lipid materials, Precirol® ATO 5 (glyceryl palmitostearate) and Transcutol® HP (diethylene glycol monoethyl ether), were received as free samples from Gattefossé SAS (Saint Priest, Cedex, France). The stabilizers, Solutol® HS 15 (polyethylene glycol 660 12-hydroxystearate) and Lutrol® F68 (Poloxamer 188) were received from BASF AG (Ludiwigshafen, Germany), whereas Tween® 80 (polyoxyethylene sorbitan monooleate) was acquired from Uniqema (Everberg, Belgium) and HPLC-grade water was obtained from a Milli Q Plus (Millipore system, Schwalbach, Germany).

Feasibility of using hot high-pressure homogenization

Before initiating formulation development studies of DDI-loaded NLC, it was considered essential to investigate the thermal stability of DDI to determine the feasibility of using hot high-pressure homogenization (HHPH) to produce the NLC formulations. Thermal gravimetry analysis (TGA) has been previously used and recommended as a simple and rapid method to determine the thermal stability of APIs[27–29]. Consequently, the thermal stability of DDI was investigated using a Model TG-DTA analyzer (Mettler-Toledo GmbH Analytical, Gießen, Germany). The sample (11.2820 mg) was weighed directly into an aluminum oxide crucible pan and heated from 30°C to 500°C at a heating rate of 10 K/min, under nitrogen by constant purging with liquid nitrogen at a flow rate of 80 mL/min.

Production of NLC formulations

The composition of the formulations that were developed and evaluated in these studies is summarized in Table 1. Aqueous DDI-free and DDI-loaded NLC were manufactured using a discontinuous HHPH[16]. In brief, DDI was dissolved in a binary lipid mixture of Precirol® ATO 5 and Transcutol® HP previously heated to 85°C. Solutol® HS 15 and Tween® 80 were added to the lipid phase to enhance the solubility of DDI in the lipid medium. An aqueous phase containing Lutrol® F68 was

heated to the same temperature as the lipid phase, and the hot aqueous phase was then dispersed in the hot lipid phase using a Model T25 Ultra-Turrax T25 homogenizer (Janke & Kunkel GmbH and Co KG, Staufen, Germany) for 1 minute with the speed set at 8000 rpm to produce a pre-emulsion. The pre-emulsion that had been formed was then homogenized using a Micron Lab 40 high-pressure homogenizer (APV Homogenizers, Unna, Germany) by applying three homogenization cycles at 800 bar. The hot oil-in-water nanoemulsion obtained was immediately filled and sealed into siliconized glass vials and allowed to cool down at room temperature (25°C) to permit subsequent recrystallization of the lipid phase and formation of NLC in situ. All samples were kept at room temperature for 24 hours prior to further characterization.

Characterization of NLC formulations

Particle size and polydispersity index

Photon correlation spectroscopy (PCS) was used to measure the mean PS and polydispersity index (PI) of the NLC formulations using a Nanosizer ZS (Malvern Instruments Ltd., Worcestershire, UK). All samples were diluted with a fixed amount of double-distilled water to obtain a suitable scattering intensity, before PCS analysis, and were then placed in a 10-mm diameter cell. Ten PCS measurements were performed for each sample at an angle of 90° at room temperature (25°C). PS analysis was performed using Mie theory with the real and imaginary refractive indices set at 1.456 and 0.01, respectively.

Laser diffractometry (LD) was used to determine the possible presence of microparticles in the NLC formulations using a Model 2000 Mastersizer laser diffractometer (Malvern Instruments Ltd.) by applying polarization intensity differential scattering. The LD data were evaluated in terms of volume distribution diameters of d50%, d90%, d95%, and d99% and by calculating span values. The span value is a statistical parameter that may be used to evaluate the PS distribution of LD data and was calculated using Equation (1).

$$\text{Span value} = \frac{\text{LD90} - \text{LD10}}{\text{LD50}}. \quad (1)$$

Zeta potential analysis

The zeta potential (ZP) was evaluated for all the NLC formulations using a Nanosizer ZS (Malvern Instruments Ltd.) in double-distilled water with conductivity adjusted to 50 μS/cm using 0.9% (w/v) sodium chloride solution at applied field strength of 20 V/cm. The ZP values were automatically generated by the Zetasizer using the Helmholtz–Smoluchowski equation.

Degree of crystallinity and polymorphism

The degree of crystallinity and polymorphism of bulk materials and the NLC formulations were investigated using a Model DSC 821^e Mettler-Toledo Differential Scanning Calorimetry (DSC) (Mettler-Toledo GmbH Analytical). The bulk lipid materials (1–2 mg) and DDI (1.4890 mg) were weighed directly and hermetically sealed into 40-μL pin-holed aluminum pans, and the DSC curves were recorded by heating the sample from 25°C to 85°C or from 25°C to 225°C, and then cooling from 85°C to 25°C or from 225°C to 25°C, respectively. A heating and cooling rate of 10 K/min was used for these studies. The DSC thermograms for all the NLC formulations were recorded by weighing between 5 and 10 mg of NLC corresponding to 1 and 2 mg of the lipid phase. An empty pin-holed aluminum pan sealed in a similar manner to the pans containing the samples for analysis was used for reference purposes. The DSC parameters, such as temperature onset, maximum peak, and enthalpy, were generated using Mettler-Toledo STARE^e software (Mettler-Toledo GmbH Analytical). The crystallinity indices of the NLC formulations under investigation were calculated using Equation (2).

$$\text{CI}(\%) = \frac{\Delta H_{\text{NLC}}}{\Delta H_{\text{bulk}} \times \text{Lipid concentration}} \times 100. \quad (2)$$

To achieve adequate interpretation of DSC data, the wide-angle X-ray scattering (WAXS) was used as a complementary analytical tool to assess the degree of crystallinity and polymorphism of bulk materials and the NLC formulations. WAXS patterns were generated using a Model PW 1830 Philips WAXS system (Philips Industrial & Electron-Acoustic Systems Division, Amedo, The

Table 1. Percentage composition (%, w/w) for NLC formulations developed and tested in these studies.

Material	DDI-free NLC	DDI-NLC 01	DDI-NLC 02	DDI-NLC 03	DDI-NLC 04	DDI-NLC 05
DDI	–	0.0150	0.0200	0.0500	0.125	0.250
Tween®80	1.00	1.00	1.00	1.00	1.00	1.00
Lutrol®F68	2.00	2.00	2.00	2.00	2.00	2.00
Solutol®HS 15	3.00	3.00	3.00	3.00	3.00	3.00
Transcutol®HP	5.00	5.00	5.00	5.00	5.00	5.00
Precirol®ATO 5	15.0	15.0	15.0	15.0	15.0	15.0
Aqua ad.	100	100	100	100	100	100

DDI loading represent a fraction of the total lipid content (DDI, Precirol®ATO 5, and Transcutol®HP).

Netherlands) equipped with a copper anode (Cu-Kα radiation, 40 kV, 25 mA λ = 0.15418 nm) coupled with a Model PW18120 Goniometer detector. All measurements were recorded using a step width of 0.04°, a count time of 60 seconds, a 2θ scanning range, and speed set between 0.6–40°and 0.02° per second, respectively. Powdered samples were mounted directly onto a glass fiber, but the measurements of the aqueous NLC dispersions were preceded by mixing the NLC sample with locust bean gum powder to produce a paste. All samples used for WAXS analysis were the same as those used in DSC analysis for the ease of data comparison and interpretation. Bragg's equation (Equation 3) relates the wavelength (λ) of the X-ray beam to both the angle of incidence (θ) and the interatomic distance (d) and was used to transform the data from scattering to the distance of spacing within a lipid matrix to obtain information about lipid modification.

$$d = \frac{\lambda}{\sin 2\theta}. \quad (3)$$

Encapsulation efficiency

The encapsulation efficiency (EE) of NLC for DDI was determined by ultrafiltration using Centrisart filter tubes (Sartorius AG, Goettingen, Germany), which consisted of a filter membrane with a molecular weight cut-off of 300 kDa at the base of the sample recovery chamber. One milliliter aliquot of undiluted sample of DDI-loaded NLC was placed in the outer chamber and the sample recovery chamber was fitted on top of the sample. The unit was closed and centrifuged at 17,000 × *g* for 30 minutes using a Model 22 R Biofuge Heraeus Sepatech centrifuge (Heraeus Sepatech GmbH, Osterode/Harz, Germany). The principle behind this process was that DDI-loaded NLC were separated from the aqueous phase and remained in the outer chamber, and the aqueous phase filtered into the sample recovery chamber through the membrane. The amount of DDI in the aqueous phase was estimated by a validated RP-HPLC. The separation of DDI and acyclovir as the internal standard was achieved using a Beckman® 60Å, 4 µm (4.0 i.d. × 150 mm) analytical column packed with a dimethyl octylsilyl (C_8)-bonded amorphous silica stationary phase. The mobile phase consisted of a binary mixture of MeOH and 25 mM potassium dihydrogen phosphate (KH_2PO_4) buffer (pH 6.0) in a ratio of 8:92 and the separation was conducted at a flow rate of 1 mL/min. The samples were monitored with UV detection at a wavelength of 248 nm and the retention time of acyclovir and DDI were 4.20 and 11.32 minutes, respectively. The total run time for the analysis was approximately 13 minutes. The amount of encapsulated active was calculated using Equation (4) by taking the difference between the total amounts used to prepare the systems and the amount of DDI that remained in the aqueous phase following the ultrafiltration process.

$$\text{EE} = \frac{(\text{Total amount of DDI}) - (\text{Free amount of DDI})}{\text{Total amount of DDI}} \times 100. \quad (4)$$

Transmission electron microscopy

The shape and the surface morphology of aqueous dispersions of NLC were investigated using a Model JEOL-1210 transmission electron microscope (JEOL 1210, JEOL Inc., Boston, MA, USA). In brief, each sample was placed on a copper grid with a carbon film and following the removal of excess liquid using a hydrophilic filter membrane, the sample was allowed to dry at 25°C for 30 seconds. The sample was then stained with 1% (w/w) phosphotungstic acid and the stain was allowed to dry at 25°C for an additional 30 seconds, after which the sample was viewed under the transmission electron microscopy (TEM) to obtain two-dimensional images of the NLC in the formulations tested.

Results and discussion

Feasibility of using high-pressure homogenization

The HHPH technique[16] was selected as the preferred method for the preparation of the NLC formulations at a production temperature of 85°C. It was anticipated that the use of the relatively high temperature could lead to the destruction of DDI, if the drug were thermolabile. There is dearth of data describing the thermal stability of DDI when the drug is exposed to relatively high temperatures. Consequently, TGA was used to establish the thermal stability of DDI, and therefore to determine the feasibility of using HHPH to produce DDI-loaded NLC. TGA has been previously used to determine the thermal stability of various drugs[27–29]. TGA profile of bulk DDI depicting the percentage weight loss of the DDI as a function of increasing temperature at a constant rate is shown in Figure 2. The percentage of weight loss of DDI

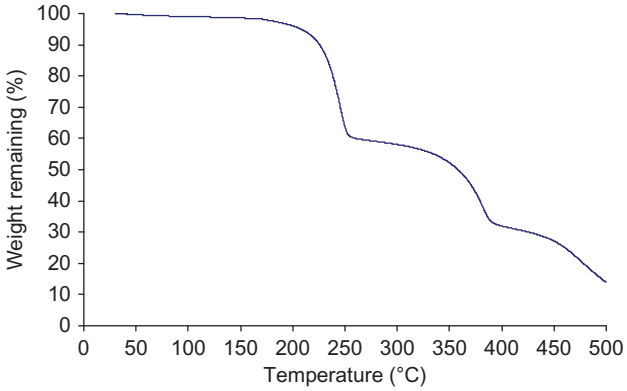

Figure 2. TGA profile of bulk DDI showing the percent weight loss of DDI as a function of increasing temperature.

following exposure of the drug to temperatures ranging between 30°C and 500°C at a heating rate of 10 K/min is summarized in Table 2.

TGA measures the loss in weight of an API sample as a function of increasing temperature, and this weight loss is then correlated to the thermal stability of an API[27–29]. TGA data show that only 1.5% of the initial weight of DDI is lost when the drug is exposed to temperatures ranging between 37°C and 163°C; however, a total of 84.1% of the initial weight of DDI is lost when the drug is heated to temperatures ranging between 163°C and 500°C. In fact, the initial weight loss of 1.5% in the temperature range between 37°C and 163°C may be attributed to water loss because DDI is slightly hygroscopic when stored at 25°C for 8 weeks[5]. Nevertheless, DDI appears to decompose in a process involving three stages as the temperature to which the drug sample is exposed exceeds 163°C (Table 2). The objective of these studies was to investigate whether DDI was thermolabile when exposed to temperatures between 75°C and 85°C, which is the temperature range the molecule would be exposed to during the production NLC. These data reveal that DDI is stable under the proposed processing and production as the drug does not exhibit significant weight loss under these conditions. Consequently, DDI-loaded NLC could be manufactured using HHPH technique.

Production of NLC formulations

DDI is highly hydrophilic (27.3 mg/mL) and therefore the solubility of the drug in lipid medium was expected to be limited. Following solubility studies, Precirol® ATO 5 and Transcutol® HP showed the best solubilizing potential for DDI and were therefore selected as solid- and liquid lipids, respectively, required for the formulation of NLC. A combination of three nonionic surfactants, namely, Solutol® HS 15, Lutrol® F68, and Tween® 80 was necessary to produce stable aqueous NLC dispersions, possibly because of the high concentration of the lipid phase (20%, w/w) used in these studies.

The use of a HHPH to produce NLC requires that an appropriate pressure and number of homogenization cycles be used to produce nanoparticles in the desirable PS range[18]. NLC dispersions were produced in these studies at a relatively high pressure of 800 bars because of the high concentration (20%, w/w) of lipid used. The number of homogenization cycles was varied, and Figure 3 depicts the effect of increasing the number of homogenization cycles on the PS and PI of DDI-free and batch DDI-NLC 04 as determined using PCS. These data reveal that increasing the number of homogenization cycles during the production process leads to a decrease in the mean particles size and narrowing of the PI for the formulations tested.

The PS of these formulations as a function of homogenization cycle was also determined using LD and these data are shown in Figure 4. These results once again show a decline in the d50%, d90%, d95%, and d99% data as the number of homogenization cycles was increased from one to three cycles.

It is therefore clear that the application of three homogenization cycles at 800 bar was sufficient to allow for the generation of enough energy to reduce the lipid droplets in the pre-emulsion to nanoparticles. Therefore, all NLC formulations were produced using a HHPH procedure using a pressure of 800 bar and three homogenization cycles, unless otherwise stated.

Table 2. Summary of percent weight loss following TGA analysis of DDI as a function of temperature.

Temperature range (°C)	DDI percentage weight loss (%)	Observation
37–163	1.5	Possible water loss
163–278	39.3	First decomposition phase
298–410	27.0	Second decomposition phase
420–500	16.3	Third decomposition phase

Characterization of NLC formulations

Aqueous DDI-NLC formulations were manufactured using increasing amounts of DDI (Table 1) to investigate the influence of DDI on the physicochemical properties of the nanoparticles that were produced. The PS and its distribution (PI and span value), ZP, and EE for NLC formulations were measured following storage of the formulations for 1 day and 2 months at 25°C and data generated from these studies are summarized in Table 3.

Particle size and polydispersity index

The measurement of PS and PI of NLC dispersions is essential to ensure the production of a stable product of suitable quality. One day following production, PCS data show that the mean PS of DDI-free and DDI-loaded NLC was between 123 and 212 nm with a low PI. An increase in the amount of DDI into NLC formulations did not have any influence on the PS and PI of the formulations. These findings are in agreement with reported data,

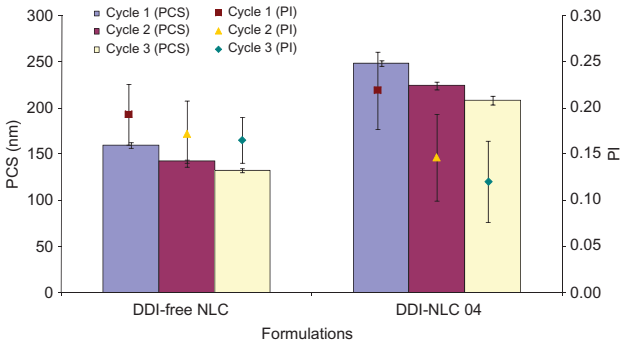

Figure 3. Effect of homogenization cycles on the mean PS and PI of DDI-free and batch DDI-NLC 04 determined using photon correlation spectrometry. Symbols with RSD bars represent the PI for each formulation.

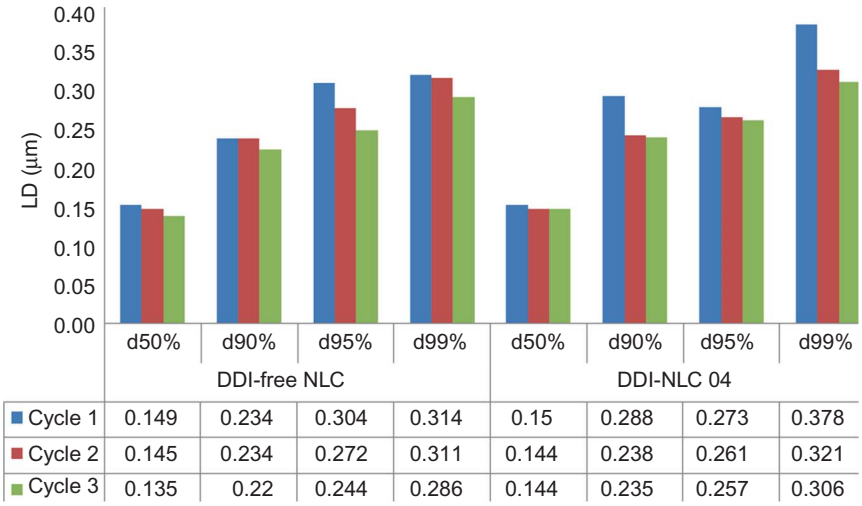

Figure 4. Effect of number of homogenization cycles on the d50%, d90%, d95%, and d99% of DDI-free and batch DDI-NLC 04 assessed using laser diffractometry.

which showed that loading concentrations of *trans*-retinoic acid had no influence on the PS of SLN[30]. LD data show that the d99% values are below 350 nm indicating that microparticles were not present in these NLC dispersions. Once again, an increase in the amount of DDI added to the formulation had no effect on the LD data. In addition, the span values for all formulations are relatively low, suggesting a narrow PS distribution and supporting the PI data that were obtained using PCS. It is also clear that PCS and LD data show that the sizes of the particles in all the formulations remained within the nanometer range following storage for 2 months at 25°C. Furthermore, the PI and span values remained low during the 2-month storage periods, indicating that there was little or no aggregation or coalescence of the particles during the storage period. Therefore, these results reveal that all NLC formulations developed in these studies were physically stable in terms of PS and its distribution for at least 2 months.

Zeta potential analysis

The ZP values for DDI-free and DDI-loaded NLC formulations manufactured with increasing amounts of DDI were generated using water as the dispersion medium

Table 3. Particle size (PCS and LD), its distribution (PI and span value), zeta potential, and encapsulation efficiency data for NLC following storage at 25°C for 1 day and 2 months.

BATCH	DDI-free NLC		DDI-NLC 01		DDI-NLC 02	
Parameter	1 day	2 months	1 day	2 months	1 day	2 months
PCS[a] (nm)	132 ± 2	136 ± 7	208 ± 4	197 ± 3	212 ± 5	202 ± 6
PI[a]	0.165 ± 0.025	0.131 ± 0.016	0.120 ± 0.044	0.113 ± 0.057	0.137 ± 0.049	0.113 ± 0.046
d50% (µm)	0.135	0.139	0.150	0.150	0.142	0.149
d90% (µm)	0.234	0.226	0.235	0.234	0.248	0.225
d95% (µm)	0.272	0.254	0.261	0.258	0.287	0.249
d99% (µm)	0.311	0.299	0.306	0.304	0.380	0.292
Span value	1.19	0.825	1.08	0.967	1.25	0.872
ZP[b] (mV)	−12.4 ± 0.9	−12.5 ± 0.4	−17.0 ± 0.9	−15.0 ± 0.1	−18.4 ± 1.0	−17.6 ± 2.1
EE (%)	—	—	78.34 ± 2.44	76.20 ± 1.44	39.37 ± 1.30	38.17 ± 0.90
Formulation	DDI-NLC 03		DDI-NLC 04		DDI-NLC 05	
Parameter	1 day	2 months	1 day	2 months	1 day	2 months
PCS[a](nm)	144 ± 3	143 ± 2	123 ± 1	131 ± 4	148 ± 3	203 ± 7
PI[a]	0.158 ± 0.042	0.0969 ± 0.035	0.141 ± 0.038	0.162 ± 0.048	0.195 ± 0.037	0.321 ± 0.0586
d50% (µm)	0.139	0.139	0.137	0.137	0.149	0.141
d90% (µm)	0.206	0.204	0.202	0.203	0.232	0.230
d95% (µm)	0.228	0.225	0.223	0.223	0.283	0.253
d99% (µm)	0.269	0.262	0.262	0.263	0.308	0.304
Span value	0.840	0.791	0.870	0.825	1.00	1.04
ZP[b] (mV)	−16.6 ± 2.3	−17.6 ± 2.1	−11.4 ± 0.40	−12.2 ± 1.2	−13.3 ± 0.90	−11.7 ± 0.36
EE (%)	37.04 ± 2.56	35.12 ± 1.46	36.52 ± 1.55	34.20 ± 0.55	34.09 ± 2.41	33.02 ± 1.53

[a]Mean of 10 (n = 10). [b]Three measurements (n = 3).

and these data are also summarized in Table 3. The conductivity of the dispersion medium was adjusted to a standard value of 50 μS/cm to avoid any artifacts in the measurement of ZP values as a consequence of day-to-day variability in the conductivity of the water. All formulations produced negative ZP values; however, it is clear that the ZP values were not as negative as those recommended for NLC formulations (ZP values of ≤ −30) to be considered stable and this may be because of a shift in the shear plane of the NLC[16,18,31]. However, it is important to note that this rule applies only to colloidal systems that are stabilized by electrostatic interactions alone. These formulations were developed using a combination of three nonionic surfactants and as these impart stability to NLC dispersions by steric hindrance, the stability of formulations may be inferred. The ZP of NLC is a key parameter that can be used to predict and control the physical stability of such colloidal dispersions on long-term storage[16,18,31,32]. It is evident that the ZP values of all formulations remained constant following storage at 25°C for 2 months, suggesting that the surface properties of the particles in all formulations were not altered during the 2-month storage period and, therefore, the stability of the NLC formulations may be inferred.

Encapsulation efficiency

The EE is an important parameter that can influence drug release characteristics and must therefore form an integral part of the formulation development process[33]. It is easier to encapsulate hydrophobic molecules in NLC with high efficiency than hydrophilic drugs such as DDI because of the tendency of hydrophilic molecules to partition out of the lipid phase into the water phase during homogenization. Because of limited solubility of DDI in lipids, a small amount of DDI was added incrementally to determine the ability of the NLC to entrap DDI. These amounts were considered sufficient for the intended purpose of these studies. The EE data for DDI determined per unit weight of each NLC formulation are also summarized in Table 3 and reveal that EE of DDI decreases as the amount of DDI added was increased from 0.015% (w/w) for batch DDI-NLC 01 to 0.25% (w/w) mg for batch DDI-NLC 05. The data also show that the amount of DDI entrapped in the nanoparticles for each formulation remained constant following storage of the formulations at 25°C for 2 months, suggesting that despite the relatively low entrapment efficiency of DDI, the formulations were at least chemically stable during the storage period.

Transmission electron microscopy

TEM was used to examine the shape and surface morphology of NLC in aqueous dispersions and the images obtained from these studies are depicted in Figure 5.

The nanoparticles in all formulations except in batches DDI-NLC 01 and DDI-NLC 05 are mainly discrete entities; however, all particles, irrespective of the formulation investigated are in the nanometer range. However, the nanoparticles in batches DDI-NLC 01 and DDI-NLC 05 seemed to have formed agglomerates, which may be due to insufficient drying time of the sample during sample preparation prior to TEM analysis. NLC in DDI-free and batch DDI-NLC 02 were spherical; however, all the other formulations contain a mixture of spherical and nonspherical (anisometric) nanoparticles. The shape of solid lipid nanocarriers is dependent on the purity of the lipid used[34] and particles prepared from highly pure lipids are usually more cuboid in nature[35], whereas those obtained using chemically polydispersed lipids are typically spherical[36]. The lipid matrix used consisted of a mixture of Precirol® ATO 5 and Transcutol® HP, which suggests that the lipid matrix is chemically polydispersed. Consequently, it was expected that only spherical particles would be present in all batches and not only in DDI-free and batch DDI-NLC 02.

It should also be realized that the polymorphic nature of the lipid matrices that are used to form solid lipid nanocarriers may determine the shape of the particles, such that particles that exist in the stable β-modification assume anisometric shapes, whereas those that exist in the metastable α-polymorphic forms are usually spherical in nature[37,38]. The shapes of solid lipid nanocarriers established using TEM may be spherical[39] or nonspherical[40–42]. In these studies, TEM images reveal spherical particles for DDI-free and batch DDI-NLC 02 only indicating that the nanoparticles in these formulations exist in an α-polymorphic form. All the other formulations comprised of spherical and nonspherical particles, which indicate that the nanoparticles in these formulations coexist as the α- and β-polymorphic forms. However, the polymorphic nature and the degree of crystallinity of particles in all formulations that were developed were confirmed using DSC and WAXS.

Degree of crystallinity and polymorphism

Differential scanning calorimetry. Prior to deterring the degree of crystallinity and polymorphic modification of bulk lipids and NLC formulations, a DSC analysis of DDI was performed to obtain information relating to the melting behavior, crystalline nature, and polymorphism of DDI before and after exposing the drug to relatively high temperatures. The DSC profile of DDI obtained before and after exposing the sample to 85°C for 1 hour is depicted in Figure 6.

The DSC thermogram of DDI before heating shows the presence of two thermal events, namely, an initial exothermic event with an extrapolated onset temperature and peak maximum temperature of 44.2°C and 81.1°C, respectively (enthalpy −436.90 J/g), and an endothermic event indicating the melting event of DDI with an extrapolated onset temperature and peak maximum of 184.1°C and 187.3°C, respectively (enthalpy –143.84 J/g). The initial event is indicative of the recrystallization of

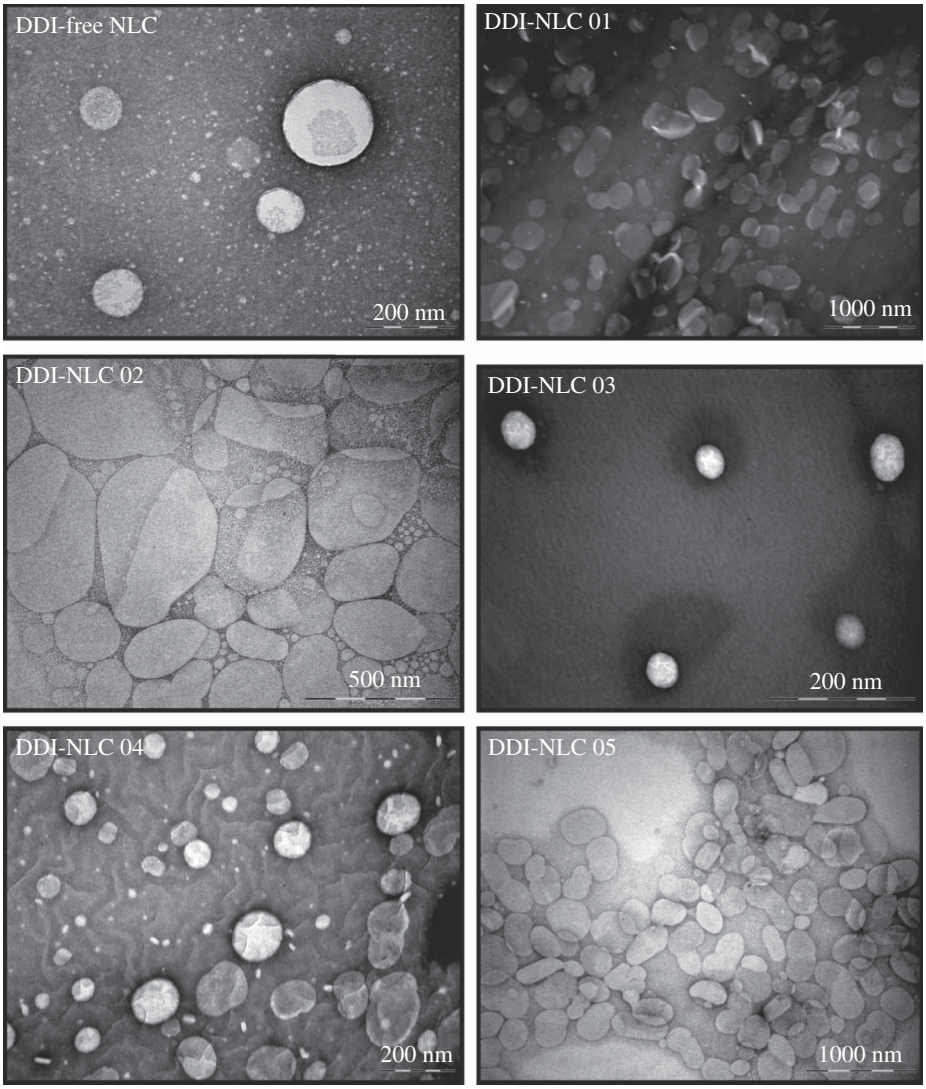

Figure 5. TEM micrographs depicting the shape and surface morphology of particles of NLC formulations.

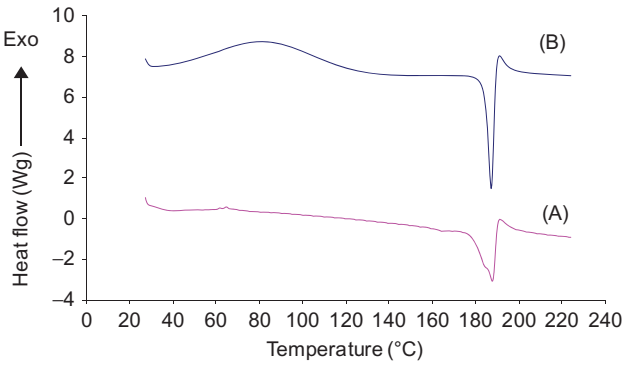

Figure 6. DSC profile for DDI prior to heat exposure (B) and following exposure to 85°C for 1 hour (A).

an unstable polymorph of DDI, and the latter event is indicative of the melting of the most stable polymorphic form of DDI. The endothermic peak is strong and sharp, which may be indicative of a high degree of crystallinity of the compound.

The exposure of DDI to 85°C for 1 hour resulted in slight changes in the melting behavior of the drug. The exothermic event is no longer evident. This may be attributed to the heat to which the drug was exposed to, prior to DSC analysis and which possibly results in the unstable polymorphic form of DDI reverting to a more stable modification of the API. Therefore, the peak is undetectable when the same sample is exposed to the same temperature range during DSC scanning.

The endothermic event exhibits both a decrease in enthalpy and the onset temperature from 143.84 J/g and 184.1°C to 134.14 J/g and 179.8°C, respectively. However, peak maximum remains constant at 187.5°C. In addition, the peak is broader and a less-intensive response compared to that observed for DDI scanned before exposure to heat. The decreased onset temperature and enthalpy in addition to the broader and less-intensive endothermic peak for DDI following heating may be attributed to a decrease in the degree of crystallinity and a change to the polymorphic nature of the more stable

Table 4. Differential scanning calorimetry parameters for NLC formulations measured following storage at 25°C for 1 day and 2 months.

Formulation	DDI-free NLC		DDI-NLC 01		DDI-NLC 02	
Parameter	1 day	2 months	1 day	2 months	1 day	2 months
Onset (°C)	48.24	48.56	51.43	50.90	50.95	50.87
MP (°C)	53.46	54.87	54.53	54.74	54.01	54.35
Enthalpy (J/g)	15.39	19.25	19.30	21.88	16.45	17.70
RI (%)	63.07	78.63	78.83	89.67	67.42	72.30
Formulation	DDI-free 03		DDI-NLC 04		DDI-NLC 05	
Parameter	1 day	2 months	1 day	2 months	1 day	2 months
Onset (°C)	49.03	49.12	48.14	48.43	48.95	48.98
MP (°)	53.59	54.30	54.54	53.72	53.90	54.73
Enthalpy (j/g)	16.16	19.29	18.92	19.87	17.04	19.79
RI (%)	45.74	78.80	77.54	81.17	69.84	80.84

polymorphic form of DDI that predominates following exposure of the drug to 85°C for 1 hour.

The polymorphic modification and the degree of crystallinity of the bulk lipid and NLC formulations were also investigated using DSC. The DSC parameters of aqueous NLC that were measured following storage at 25°C for a period of 1 day and 2 months are summarized in Table 4.

Regardless of the storage period, the onset temperatures, peak maxima (MP), and the melting enthalpies for the NLC formulations were all lower than that of the bulk lipid material, Precirol® ATO 5, which showed an onset, MP, and calculated enthalpy of 52.18°C, 55.06°C, and 122.04°C, respectively. DSC parameters of NLC formulations remained constant irrespective of the amount of DDI that was added to a formulation again suggesting the low EE for DDI. In addition, all formulations had a melting endotherm, which is indicative that the particles recrystallized and that there were no supercooled melts present in all formulations that were manufactured.

It has been established that irrespective of the composition of the lipid matrix used to manufacture solid lipid nanocarriers and/or the type of surfactants used to ensure thermodynamic stability of the system, a major factor affecting the thermal behavior of solid lipid-based carriers is the PS of the particles[43]. In other words, the onset temperature, MP, and melting enthalpy of triacylglycerol-based carriers are directly proportional to the size of the particles[43]. Consequently, the melting parameters of the nanoparticles in all formulations were lower than those of the bulk Precirol® ATO 5. With respect to storage conditions, there is a slight increase in the value of all melting parameters for all formulations when the measurements were derived from samples stored for 2 months at 25°C compared to those generated 1 day after production of the nanoparticles. This is possibly because of the fact that the lipid matrix had not recrystallized fully following storage for 1 day as confirmed by the relatively low recrystallization index (RI) values obtained for all formulations. Therefore, following production and storage for 1 day, the nanoparticles are likely to exist in the metastable α-polymorphic modification. However, after storage of the formulations for 2 months, the RI values of the particles increase relatively thereby suggesting that the particles may be reverting to the stable β-modification form from the metastable α-polymorphic form. In addition, the melting peak of DDI was not detected in DSC thermograms of all formulations indicating that any DDI that was incorporated into the NLC may be molecularly dispersed in the matrix[34]. However, it should be acknowledged that the relatively low drug loading and EE of NLC for DDI in these studies makes it difficult to draw conclusions as to the crystalline or amorphous nature of DDI in these NLC using conventional DSC alone. This is because DSC may not be a reliable analytical tool for the detection of crystallization energy of low amounts (<10%) of amorphous material in a predominantly crystalline matrix[44–46]. Consequently other analytical tools such as X-ray diffraction, that have been shown to have detection limits of 0.5% and 0.05% in some cases for crystalline materials[47], may be used to determine the crystalline nature of the low amounts of DDI in these NLC formulations.

Wide-angle X-ray scattering. WAXS was used as a complementary analytical tool to DSC to support the DSC data. The WAXS patterns of DDI prior to and following exposure of the drug to 85°C for 1 hour are depicted in Figure 7.

The WAXS profile obtained for DDI prior to and following exposure to heat shows the presence of a number of similar diffraction bands that are characteristic of crystalline substances. Consequently, these data reveal that DDI is a crystalline substance and retains its crystalline state following exposure to heat of 85°C for 1 hour. However, in general there appears to be a slight decrease in the peak intensity obtained for the DDI sample that was exposed to heat when compared to the peak intensity observed for the DDI sample that was not exposed to heat. The decrease in the intensity of the peaks of the sample exposed to heat may be attributed to a decrease in the degree of crystallinity and possibly a change in the

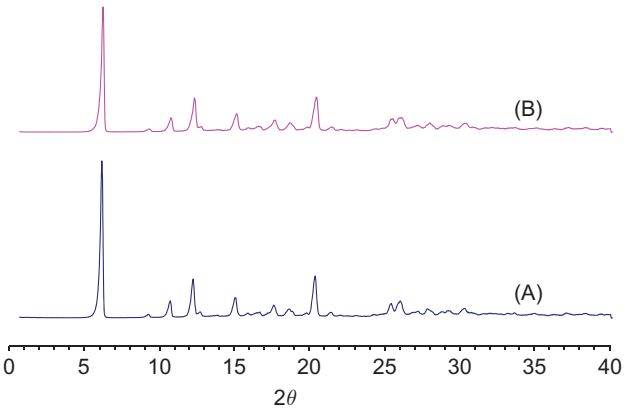

Figure 7. WAXS patterns of DDI prior to heat exposure (B) and following heating to 85°C for 1 hour (A).

polymorphic nature of DDI following heat exposure. These data support those observed in DSC studies and reveal that exposure of DDI to 85°C for 1 hour more than likely decreases the degree of crystallinity of DDI and possibly modifies the polymorphic nature of the drug, however judging Figure 7, these changes appear insignificant.

WAXS was also used to evaluate the degree of crystallinity and polymorphic modification in bulk lipid materials and NLC formulations. WAXS measures the length of the long and short spacings between alkyl side chains within an acylglyceride lipid layer and these appear as one or more reflections in the wide-angle region[18]. Lipid modifications can be identified using criteria set for X-ray diffraction patterns when the intensity is plotted against the scattering vector (s)[48,44]. An α-modification has a single scattering reflex with a Bragg's distance ranging between 0.410 and 0.420 nm, but a β′-modification has two reflexes at a Bragg's distance of 0.389 and 0.420 nm[48,44]. In addition, a β_i-modification reveals three reflexes at Bragg's distance of 0.389, 0.420, and 0.460 nm[48,44]. A lipid is said to have a β-modification if the above criteria are not met[44]. The diffraction patterns of the bulk lipid materials are shown in Figure 8 with their associated Bragg's spacing values that allows for the identification of solid lipid modifications.

Precirol® ATO 5 shows two reflections at Bragg distances of 0.416 and 0.461 nm before being exposed to heat, but a single reflection at 0.415 nm is observed after heating. These data indicate that bulk Precirol® ATO 5 possibly exists in a β-modification, but transforms to α-modification when exposed to 85°C and suggests that heating Precirol® ATO 5 leads to a less-ordered structure of the lipid matrix[44]. A bulk binary mixture of Precirol® ATO 5 and Transcutol® HP that was also subjected to 85°C for 1 hour showed reflections at various Bragg distances (Figure 6), and these results suggest the presence of a β-modification.

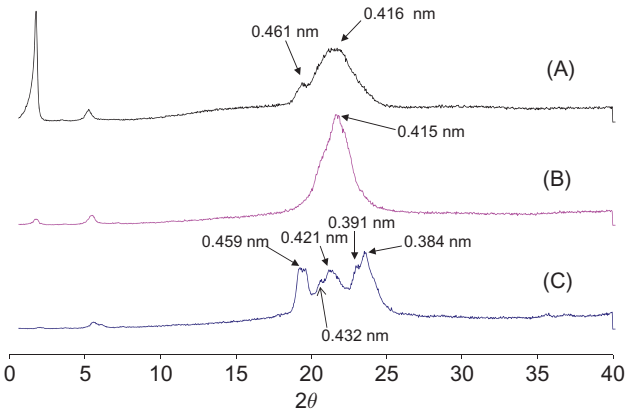

Figure 8. WAXS patterns of Precirol® ATO 5 and a binary mixture of Precirol® ATO 5 and Transcutol® HP and the corresponding Bragg spacing values, (A) Precirol® ATO 5 prior to heat exposure, (B) Precirol® ATO 5 following heat exposure, and (C) binary mixture of Precirol® ATO 5 and Transcutol® HP following heat exposure.

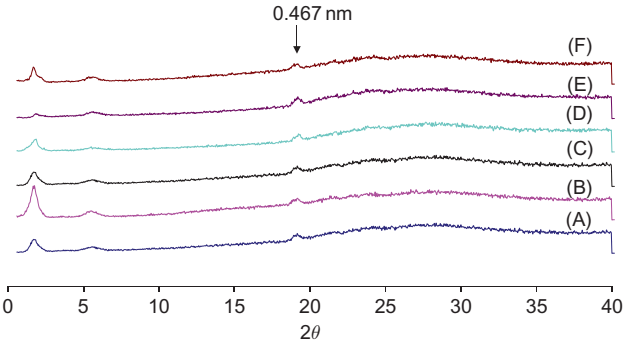

Figure 9. WAXS patterns of all developed NLC aqueous dispersions, (A) DDI-free NLC, (B) DDI-NLC 1, (C) DDI-NLC 2, (D) DDI-NLC 3, (E) DDI-NLC 4, and (F) DDI-NLC 5.

The WAXS diffraction patterns of NLC formulations generated following storage at 25°C for 1 day are shown in Figure 9. All NLC formulations (Figure 7) showed a single reflection at a Bragg's distance of 0.467, which suggest that lipid modification in the formulations is a β-modification. This modification is similar to that obtained for a binary bulk mixture of Precirol® ATO 5 and Transcutol® HP. In addition, there was no characteristic peak for DDI in all diffractograms generated for DDI-loaded NLC, which indicates that any DDI that was incorporated was incorporated in a molecularly dispersed manner, within the solid lipid matrix, which is in agreement with the data obtained using DSC. There was little difference in the degree of crystallinity of the particles following storage for 2 months (data not shown).

Conclusions

There is a need for the formulation and development of drug delivery systems that have the ability to deliver anti-HIV agents to the CNS by circumventing the BBB to adequately manage HIV infection within CNS and therefore brain dementia complex. Therefore, the objective of these studies was to investigate the feasibility of encapsulating DDI in NLC, which could be used as a potential vehicle to deliver DDI to the CNS. DDI-loaded NLC formulations were developed; however, because of the limited solubility of the compound in the lipid phase, only small amounts of API was used in these experiments.

The mean size of the particles was within the nanometer range with PCS values <250 nm and d99% values <400 nm for all NLC formulations. Furthermore, all NLC formulations had a narrow PS distribution irrespective of the amount of DDI that was added during manufacture. Imaging analysis using TEM also confirmed that the size of the nanoparticles was within the nanometer range and that particles in these formulations were spherical and/or nonspherical (anisometric). The ZP of NLC formulations ranged from −18.4 and −11.4 mV when measured 1 day after manufacture and following storage for

2 months at 25°C, indicating that the formulation were physically stable for at least 2 months after manufacture. The EE decreased with an increase in the amount of DDI loaded in NLC formulations, but remained constant following storage at 25°C for 2 months.

The results of DSC studies revealed that all formulations had a melting endotherm suggesting that the particles had recrystallized and that there were no supercooled melts present in all formulations that were manufactured. DSC analysis also revealed that the RI of the particles in all formulations was less than 100% following storage for 1 day, suggesting that the nanoparticles exist in the metastable α-polymorphic modification. However, following storage for 2 months, the RI values for particles in all formulations increased slightly, suggesting that the particles may be reverting to the stable β-modification form from the metastable α-polymorphic form. WAXS analysis revealed that NLC formulations had similar refraction patterns irrespective of the amount of DDI added and the storage period of each formulation.

These studies showed that it may be feasible to incorporate DDI into NLC, which could be used as a vehicle to deliver DDI to the brain, which could be a major breakthrough in the management of ADC. The drug loading and EE of NLC for DDI is relatively low in terms of the applicability of this drug delivery system for the treatment of ADC. Consequently, formulation strategies should be designed and implemented aimed at enhancing the drug loading and EE of the carrier for DDI to fully appreciate the full potential for the use of NLC to treat ADC. In addition, the potential for NLC to delivery DDI to the brain should be investigated in vitro and in vivo to appreciate the full extent of the usefulness of DDI-loaded NLC in the management of ADC.

Declaration of interest

The authors gratefully acknowledge the Andrew Mellon Scholarship (KWK), the Deutscher Akademischer Austausch Dienst (DAAD) (WKMK, RHM), and the Joint Research Committee of Rhodes University (RBW) for financial assistance. The authors report no conflicts of interest. The authors are responsible for the content and writing of this paper.

References

1. Sweetman SC (2002). Antivirals: Didanosine. In: Sweetman SC, ed. Martindale: the complete drug reference. London: The Pharmaceutical Press, 618–19.
2. Gibbon CJ (2008). Antivirals for systemic use: Didanosine. In: Gibbon CJ, ed. SAMF: South African Medicines Formulary. Cape Town: Health and Medical Publishing Group, 322.
3. De Clercq E. (2004). HIV chemotherapy and prophylaxis: New drugs, leads and approaches. Int J Biochem Cell Biol, 36:1800–22.
4. De Clercq E. (2004). Antiviral drugs in current clinical use. J Clin Virol, 30:115–133.
5. Nassar MN, Chen T, Reff MJ, Agharkar SN. (1993). Didanosine. In: Brittain HG, ed. Analytical profiles of drug substances and excipients. New York: Academic Press Inc., 185–227.
6. Portegies P. (1994). AIDS dementia complex: A review. J Acq Immun Def Synd, 7:S38–S49.
7. Yatvin MB, Li W, Meredith MJ, Shenoy MA. (1999). Improved uptake and retention of lipophilic prodrug to improve treatment of HIV. Adv Drug Deliv Rev, 39:165–82.
8. Portegies P, Enting RH, De Gans J, Algra PR, Derix MMA, Lange JMA, et al. (1993). Presentation of AIDS dementia complex: 10 years of follow-up in Amsterdam, The Netherlands. AIDS, 7:669–75.
9. McArthurJ.C, Selnes OA, Glass JD, Hoover DR, Bacellar H. (1994). HIV dementia: Incidence and risk factors. In: Price RW, Perry SW, eds. HIV, AIDS and the Brain. New York: Raven Press, 251–72.
10. Perices M, Cooper DA. (1990). Neuropsychological investigation of patients with AIDS and ARC. J Acq Immun Def Synd, 36:555–64.
11. Price R, Brew B. (1988). AIDS commentary: The AIDS dementia complex. J Infect Dis, 158:1079–83.
12. Brew BJ. (1999). AIDS dementia complex. Neurol Clin, 17:861–81.
13. Schrager LK, D'Souza MP. (1998). Cellular and anatomical reservoirs of HIV-1 in patients receiving potent antiretroviral combination therapy. J Am Med Assoc, 280:67–71.
14. Schwarz C, Mehnert W, Lucks JS, Müller RH. (1993). Solid lipid nanoparticles (SLN) for controlled drug delivery I. Production, characterization and sterilization. J Control Release, 30:83–96.
15. zur Mühlen A, Schwarz C, Mehnert W. (1998). Solid lipid nanoparticles (SLN) for controlled drug delivery-drug release and release mechanism. Eur J Pharm Biopharm, 45:149–55.
16. Müller RH, Mäder K, Gohla S. (2000). Solid lipid nanoparticles (SLN) for controlled drug delivery-a review of the state of the art. Eur J Pharm Biopharm, 50:161–77.
17. Müller RH, Mehnert W, Lucks JS, Schwarz C, zur Mühlen A, Wyhers H, et al. (1995). Solid lipid nanoparticles (SLN): An alternative colloidal carrier system for controlled drug delivery. Eur J Pharm Biopharm, 41:62–69.
18. Mehnert W, Mäder K. (2001). Solid lipid nanoparticles: Production, characterization and applications. Adv Drug Deliv Rev, 47:165–96.
19. Müller RH, Radtke M, Wissing SA. (2002). Nanostructured lipid matrices for improved microencapsulation of drugs. Int J Pharm, 242:121–28.
20. Radtke M, Souto EB, Müller RH. (2005). Nanostructured lipid carriers: A novel generation of solid lipid drug carriers. Pharm Tech Eur, 17:45–50.
21. Radtke M, Müller RH. (2001). Nanostructured lipid carriers. New Drugs, 2:48–52.
22. Müller RH, Radtke M, Wissing SA. (2002). Solid lipid nanoparticles (SLN) and nanostructured lipid carriers (NLC) in cosmetic and dermatological preparations. Adv Drug Deliv Rev, 54:S131–55.
23. Wissing SA, Kayser O, Müller RH. (2004). Solid lipid nanoparticles for parenteral drug delivery. Adv Drug Deliv Rev, 58:1257–72.
24. Pal Kaur I, Bhandari R, Bhandari S, Kakkar V. (2007). Potential of solid lipid nanoparticles in brain targeting. J Control Release, 127:97–109.
25. Müller RH, Keck CM. (2004). Drug delivery to the brain-realization by novel drug carriers. J Nanosci Nanotechnol, 4:471–83.
26. Göppert TM, Müller RH. (2005). Polysorbate-stabilized solid lipid nanoparticles as colloidal carriers for intravenous targeting of drugs to the brain: Comparison of plasma protein adsorption patterns. J Drug Target, 13:179–87.
27. Souto EB, Anselmi C, Centini M, Müller RH. (2005). Preparation and characterization of n-dodecyl-ferulate-loaded solid lipid nanoparticles (SLN®). Int J Pharm, 295:261–68.
28. Teeranachaideekul V, Souto EB, Müller RH, Junyaprasert V. (2008). Physicochemical characterization and *in vitro* release studies of ascorbyl palmitate-loaded semi-solid nanostructured lipid carriers (NLC gels). J Microencapsulation, 25:111–20.
29. Souto EB, Müller RH. (2005). SLN and NLC for topical delivery of ketoconazole. J Microencapsulation, 22:501–10.

30. Lim SJ, Kim CK. (2002). Formulation parameters determining the physicochemical characteristics of solid lipid nanoparticles loaded with all-trans retinoic acid. Int J Pharm, 243:135–46.
31. Heurtault B, Saulnier P, Pech B, Proust JE, Benoit JP. (2003). Physicochemical stability of colloidal lipid particles. Biomaterials, 24:4283–300.
32. Radomska-Soukharev A. (2007). Stability of lipid excipients in solid lipid nanoparticles. Adv Drug Deliv Rev, 59:411–18.
33. Joshi M, Patravale V. (2007). Nanostructured lipid carrier (NLC) based gel of celecoxib. Int J Pharm, 346:124–32.
34. Teeranachaideekul V, Souto EB, Junyaprasert VB, Müller RH. (2007). Cetyl palmitate-based NLC for topical delivery of Coenzyme Q10 – Development, physicochemical characterization and *in vitro* release studies. Eur J Pharm Biopharm, 67:141–48.
35. Westesen K, Siekmann B, Koch MHJ. (1993). Investigations on the physical state of solid lipid nanoparticles by synchrom radiation X-ray diffraction. Int J Pharm, 93:189–99.
36. Dingler A, Blum RP, Niehus H, Müller RH, Gohla S. (1999). Solid lipid nanoparticles (SLN/Lipopearls): A pharmaceutical and cosmetic carrier for the application of vitamin E in dermal products. J Microencapsulation, 16:751–67.
37. Souto EB, Müller RH. (2006). Investigation of the factors influencing the incorporation of clotrimazole in SLN and NLC prepared by hot high-pressure homogenization. J Microencapsulation, 23:377–88.
38. Schubert MA, Müller-Goymann CC. (2005). Characterization of surface-modified solid lipid nanoparticles (SLN): Influence of lecithin and non-ionic emulsifier. Eur J Pharm Biopharm, 61:77–86.
39. Saupe A, Wissing SA, Lenk A, Schmidt C, Müller RH. (2005). Solid lipid nanoparticles (SLN) and nanostructured lipid carriers (NLC)-structural investigations on two different carrier systems. Biomed Mater Eng, 15:393–402.
40. Luo Y, Chen D, Ren L, Zhao X, Qin J. (2006). Solid lipid nanoparticles for enhancing vinpocetine's oral bioavailability. J Control Release, 114:53–59.
41. Ugazio E, Cavalli R, Gasco MR. (2002). Incorporation of cyclosporin A in solid lipid nanoparticles (SLN). Int J Pharm, 241:341–44.
42. Liu J, Hu W, Chen H, Ni Q, Xu H, Yang X. (2007). Isotretinoin-loaded solid lipid nanoparticles with skin targeting for topical delivery. Int J Pharm, 328:191–95.
43. Wissing SA, Müller RH, Manthei L, Meyer C. (2004). Structural characterization of Q10-loaded solid lipid nanoparticles by NMR spectroscopy. Pharm Research, 21:400–05.
44. Müller RH, Runge SA, Ravelli V, Thünemann AF, Mehnert W, Souto EB. (2008). Cyclosporine-loaded solid lipid nanoparticles (SLN®): Drug-lipid physicochemical interactions and characterization of drug incorporation. Eur J Pharm Biopharm, 68:535–44.
45. Saunders M, Podluii K, Shergill S, Buckton G, Royall P. (2004). The potential of high speed DSC (Hyper-DSC) for the detection and quantification of small amounts of amorphous content in predominantly crystalline samples. Int J Pharm, 274:35–40.
46. Saklatvala R, Royall PG, Craig DQM. (1999). The detection of amorphous material in a nominally crystalline drug using modulated temperature DSC – A case study. Int J Pharm, 192:55–62.
47. PANanlytical application notes. (2010). Crystallinity determination: quantification of low amounts of amorphous material in a crystalline matrix and vice versa. The Netherlands: PANanalytical B.V. http://www.xrdml.com/index.cfm?pid=224&itemID=162&contentItemID =114 [accessed April 8, 2010].
48. Hernqvist L. (1988). Crystal structures of fats and fatty acids. In: Garti N, Sato K, eds. Crystallization and polymorphism of fats and fatty acids. New York: Marcel Dekker Inc., 97–137.